

Geometric theory of quark confinement

Alexander Migdal^{a,*}

^a*Institute for Advanced Study, Princeton, USA*

Abstract

We present the nonperturbative solution of the loop equation in quenched QCD (one quark loop in full gluon vacuum, including nonplanar graphs). This solution relies on a specific local minimum of the Plateau problem—one that is additive over the closed parts of the bounding loop formed at self-intersections. This surface applies to large loops, leading to quark confinement via a factor $\exp(-\kappa S[C])$ multiplying the perturbative Wilson loop $W_{pert}[C]$. Crucially, the confinement mechanism relies on the self-duality of the area derivative—a property that exists exclusively in four dimensions. This geometric constraint ensures stability only in four dimensions, distinguishing the resulting spectrum from standard string models, which are stable only in higher embedding dimensions. We compute the high-energy meson spectrum resulting from this novel confinement mechanism. The result is a usual linear Regge trajectory with the slope $\alpha' = \frac{1}{2\pi\sigma}$ in our normalization of string tension $\sigma = 2\sqrt{2}\kappa$. However, there are no string modes to be added to the spectrum in our solution, which amounts to the static linear potential for the quark pair. As we argue, the fluctuations of "flux tube" between quarks are accounted for in the gluon diagrams in $W_{pert}[C]$, and do not contribute to the confining force. This eliminates the problems of quantization of string in four dimensions.

1. Introduction

In this paper we consider the $N_f \rightarrow 0$ (quenched) valence limit of QCD at fixed N_c . The vacuum is pure Yang–Mills; quark currents are represented by a single closed valence quark loop whose propagation amplitude is multiplied by the Wilson loop $W[C]$ in the gluonic vacuum. In this limit, hadronic states cannot decay by creating additional $q\bar{q}$ pairs, and the meson spectrum is purely confining (rising to infinity). We approximate $W[C]$ by the Hodge–dual factor $\exp(-\kappa S[C])$, neglecting subleading gluon–graph corrections in the large–loop limit. This factor, as we argue in this work, represents an exact solution of the MM chain of multi-loop equations [1, 2, 3].

We specifically analyze a helical loop configuration (the Helicoid), which allows for an analytic WKB computation of the meson mass at large angular momentum, where the radius of the helix is large.

2. Self-dual area derivative and loop equation

Let us remind why we are looking for the self-dual minimal surface, as suggested in [4]. The area derivative for a general functional $W[C]$ was

defined in that paper as a discontinuity of the second variation of the area

$$\frac{\delta W}{\delta\sigma_{\mu\nu}(\theta)} = \frac{\delta^2 W}{\delta C'_\mu(\theta-0)\delta C'_\nu(\theta+0)} - \mu \leftrightarrow \nu \quad (2.1)$$

The loop equation for the Yang–Mills gradient flow was shown in [4] to reduce to the loop space diffusion equation, which allows the solution $W = \exp(-\kappa S[C])$ provided that $S[C]$ is a zero mode of this equation

$$\mathcal{L}(S) = 0; \quad (2.2)$$

$$\mathcal{L} = \oint_\theta C'_\nu(\theta) \left(\frac{\delta}{\delta C'_\mu(\theta+0)} - \frac{\delta}{\delta C'_\mu(\theta-0)} \right) \frac{\delta}{\delta\sigma_{\mu\nu}(\theta)} \quad (2.3)$$

The basic observation made in that paper was that there is an SD solution similar to the Yang–Mills multi-instanton. The loop space diffusion equation (2.3) is identically satisfied for any functional $S[C]$ with SD or ASD area derivative

$$* \frac{\delta S}{\delta\sigma_{\mu\nu}(\theta)} = \pm \frac{\delta S}{\delta\sigma_{\mu\nu}(\theta)}; \quad (2.4)$$

$$e_{\alpha\mu\nu\lambda} \left(\frac{\delta}{\delta C'_\alpha(\theta+0)} - \frac{\delta}{\delta C'_\alpha(\theta-0)} \right) \frac{\delta S}{\delta\sigma_{\mu\nu}(\theta)} \equiv 0; \quad (2.5)$$

The last equation (Bianchi identity) is valid at the kinematical level as a Jacobi identity for a triple commutator (see [4] for a proof). The matrix in the Dirichlet boundary conditions (BC) for $X \sim QC$ should be chosen so that the area derivative

*Corresponding author

Email address: amigdal@ias.edu (Alexander Migdal)

represents the SD or ASD tensor. This choice would make the exponential of the Hodge-dual minimal area an exact solution to the loop equation.

The existence of this zero mode is heavily based on the so called Leibniz property of the loop operator and similar singular loop operators in loop calculus.

$$\mathcal{L}f(\Phi[C]) = f'(\Phi[C])\mathcal{L}\Phi[C]; \quad (2.6)$$

$$\mathcal{L}(A[C]B[C]) = \mathcal{L}(A[C])B[C] + A[C]\mathcal{L}(B[C]) \quad (2.7)$$

It was heuristically claimed in the original MM papers [2, 3], and rigorously proven in the loop calculus [4], section 3, eqs (39), (40). Due to the Leibnitz property,

$$\begin{aligned} \mathcal{L}(\exp(-\kappa S[C])W_0[C]) &= \\ -\kappa\mathcal{L}(S[C])\exp(-\kappa S[C])W_0[C] &+ \\ +\exp(-\kappa S[C])\mathcal{L}(W_0[C]) &= \exp(-\kappa S[C])\mathcal{L}(W_0[C]) \end{aligned} \quad (2.8)$$

We are looking for such a self-dual minimal surface which is *additive* at the self-intersecting loops. This condition will be discussed in detail below. It is *crucial* for the whole theory— due to this additivity the confining factor $\exp(-\kappa S[C])$ is compatible with the whole chain of the loop equations.

2.1. Compatibility with the MM loop equations.

The full chain of loop equations for the Wilson loops with a finite number of colors N_c [2, 3] has the same loop operator (2.3) as the Yang–Mills gradient flow, except there is no time derivative. In this paper, we are only considering the full chain of the multiloop equations for QCD, and **not** the Yang–Mills gradient flow equations. We use, however, the **loop calculus** developed in that paper, as it applies to the loop diffusion operator (2.3), which is the same in the multiloop MM chain and in the Yang–Mills gradient flow equation. It has the structure

$$\mathcal{L}(W_n) = K_1(W_{n+1}) + K_2(W_n) + K_3(W_{n-1}) \quad (2.9)$$

Where the integral operator $K_{1,2,3}$ involves δ functions for intersections of the loop. There are either self-intersections or intersections between the loop, and the three terms correspond to the cases when loops are either split into two pieces at the intersections (W_{n+1} case) or remain intact (W_n case), or when two loops join into one loop (W_{n-1} case). The operators $K_{1,2,3}$ all involve the following bilocal kernel

$$\iint d\theta_1 d\theta_2 C'_i(\theta_1) \cdot C'_j(\theta_2) \delta(C_i(\theta_1) - C_j(\theta_2)) \dots$$

. Under $\theta_a = \phi_a(\tau_a)$ (with $\phi'_a > 0$),

$$\begin{aligned} d\theta_a C'_i(\theta_a) &= d\tau_a \dot{C}_i(\tau_a), \\ \delta(C_i(\theta_1) - C_j(\theta_2)) &= \delta(C_i(\phi_1(\tau_1)) - C_j(\phi_2(\tau_2))), \end{aligned} \quad (2.10)$$

So, the kernel is parameterization-invariant. Therefore, the canonical standardization to $[0, 2\pi]$ used above is legitimate and additivity of $S[C]$ guarantees that the multiplicative dressing $W \mapsto W \exp(-\kappa S)$ preserves the MM factorization $\mathcal{L}W[C_1 \circ C_2] = W[C_1] \otimes W[C_2]$ whenever $\mathcal{L}S = 0$ (see (2.3) and [3, 4]).

Let us stress that this factorization takes place *independently* of the splitting points θ_1, θ_2 . Thus, for every θ_1, θ_2 , the product of two factors $\exp(-\kappa S[C_1])$ and $\exp(-\kappa S[C_2])$ exactly equals the factor $\exp(-\kappa S[C])$ on the left side of the MM equation; thus, it can be taken out of the integral, after which it cancels on both sides of the MM equation.

Clarification of the Solution Status. It is important to distinguish the mathematical status of the dressing mechanism from its physical interpretation. **Theorem 2.1** below establishes an *exact symmetry* of the MM hierarchy: the dressing transformation $W \rightarrow W \cdot \exp(-\kappa S[C])$ maps any solution of the loop equations to another exact solution, provided $S[C]$ is a strictly additive zero-mode.

The *physical hypothesis* of this paper is that the actual gluonic vacuum of QCD is described by this dressed solution, choosing the perturbative vacuum W_{pert} as the seed. While the symmetry is exact, the separation into a perturbative factor and a purely geometric area law is physically most distinct in the *large-loop limit*, where the area term dominates. For small loops, the interplay between the perturbative series (and its renormalons) and the non-perturbative parameter κ becomes complex, as discussed in Remark 5.3 regarding the Borel summation.

2.2. Confining factor in the multiloop hierarchy

Theorem 2.1 (Finite- N_c dressing symmetry). *Let $\{W_n\}_{n \geq 1}$ denote the n -loop Wilson loop averages in pure $SU(N_c)$ Yang–Mills theory, satisfying the MM multiloop hierarchy [3]. Let $S[C]$ be the geometric functional constructed above, with the properties*

1. $LS = 0$, where L is the loop diffusion operator (2.3);
2. *strict additivity at intersections: whenever a loop C self-intersects at $x = y$ into subloops C_{xy} and C_{yx} , one has*

$$S[C] = S[C_{xy}] + S[C_{yx}],$$

and similarly for intersections between distinct loops.

For any real positive parameter κ , define the multiplicatively dressed correlators

$$\begin{aligned} \widetilde{W}_n(C_1, \dots, C_n) \\ := W_n(C_1, \dots, C_n) \exp\left(-\kappa \sum_{i=1}^n S[C_i]\right). \end{aligned} \quad (2.11)$$

Then, for any finite N_c , the family $\{\widetilde{W}_n\}$ also satisfies the full MM multiloop hierarchy with the same N_c .

Proof. The same loop operator L in (2.3) appears on the left-hand side of the general QCD loop equations [3] for arbitrary N_c . The difference between the planar and finite- N_c cases lies only in the right-hand side: at a self-intersection, the planar factorization is replaced by a combination of one- and two-loop averages, but the kernel of the bilocal integral is the same.

At a self-intersection point of a single loop C , the finite- N_c loop equation involves the combination:

$$W_2[C_{xy}, C_{yx}] - \frac{1}{N_c^2} W_1[C_{xy} \circ C_{yx}].$$

This equation is one link in the chain relating W_n to $W_{n\pm 1}$; for finite N_c the chain terminates due to the Fierz identity for $SU(N_c)$ [3], a fact recently exploited in lattice studies of the loop equation [5].

In the general multiloop case, $W_n[C^1, \dots, C^n]$, the hierarchy contains integrals over pairs of points x, y lying on two (not necessarily distinct) loops C^i, C^j , again with the standard MM kernel. When x and y lie on two distinct loops C^i and C^j , the corresponding term involves a merging of these loops in W_{n-1} at the intersection point,

$$\frac{1}{N_c^2} W_{n-1}[\dots, C_{xy}^i \circ C_{yx}^j, \dots] - W_n[\dots, C_{xy}^i, C_{yx}^j, \dots].$$

Thus, every equation in the hierarchy relates loop functionals evaluated on collections of loops that differ only by local splittings or mergings at intersection points.

Now substitute the dressing ansatz (2.11) into the multiloop hierarchy. Because $\mathcal{L}S = 0$ and \mathcal{L} is linear, the loop operator on the left-hand side passes through the exponential factor and acts only on the seed functional W_n . Identifying this seed with the perturbative solution, $W_n = W_{n,\text{pert}}$, we obtain:

$$\begin{aligned} & \mathcal{L} \widetilde{W}_n(C_1, \dots, C_n) \\ &= \exp\left(-\kappa \sum_i S[C_i]\right) \mathcal{L} W_{n,\text{pert}}(C_1, \dots, C_n). \end{aligned} \quad (2.12)$$

In particular, the dressed correlators satisfy the same differential operator \mathcal{L} as the undressed ones.

On the right-hand side, consider first a self-intersection of a single loop C . After dressing, the corresponding contribution becomes

$$\begin{aligned} & \left(W_{2,\text{pert}}(C_{xy}, C_{yx}) - \frac{1}{N_c^2} W_{1,\text{pert}}(C_{xy} \circ C_{yx}) \right) \\ & \exp(-\kappa(S[C_{xy}] + S[C_{yx}])). \end{aligned} \quad (2.13)$$

By strict additivity, $S[C] = S[C_{xy}] + S[C_{yx}]$ at the intersection point $x = y$. Thus, the exponential

factor in (2.13) is the same as the factor multiplying the left-hand side, and therefore cancels from the equation.

For an intersection of two distinct loops C^i and C^j , the right-hand side contains terms of the schematic form

$$\begin{aligned} & \left(W_{n,\text{pert}}(C_{xy}^i, C_{yx}^j) - \frac{1}{N_c^2} W_{n-1,\text{pert}}(C_{xy}^i \circ C_{yx}^j) \right) \\ & \times \exp\left(-\kappa\left(S[C_{xy}^i] + S[C_{yx}^j] + \sum_{k \neq i,j} S[C^k]\right)\right). \end{aligned} \quad (2.14)$$

Again, by additivity at the intersection and for disjoint unions,

$$\begin{aligned} & S[C^i] + S[C^j] \\ &= S[C_{xy}^i] + S[C_{yx}^i] + S[C_{xy}^j] + S[C_{yx}^j] \\ &= S[C_{xy}^i \uplus C_{yx}^j] + S[C_{yx}^j \uplus C_{xy}^i] \\ &= S[C_{xy}^i \uplus C_{yx}^j \uplus C_{yx}^j \uplus C_{xy}^i] \end{aligned} \quad (2.15)$$

so the sum $\sum_i S[C^i]$ is invariant under the local splitting/merging operation. Hence, the same exponential factor multiplies every term in the multiloop equation and cancels between the two sides.

Since this reasoning applies to each equation in the finite- N_c hierarchy and uses only (i) the universal kernel and operator \mathcal{L} and (ii) the additivity and zero-mode properties of $S[C]$, it follows that the dressed correlators \widetilde{W}_n satisfy the same multiloop MM hierarchy for any finite N_c . \square

Remark 2.1. Note that the perimeter of the set of loops is also an additive functional, factorizing over the right side of the MM chain of equations. However, this is not a Stokes-type functional, so it does not process finite area derivatives, and, as a consequence, it cannot be added to the zero mode of the loop operator \mathcal{L} . Such terms arise as quark-mass renormalization corrections in the perturbative Wilson-loop factor; they are linearly divergent and depend on the regularization scheme. In any case, these terms do not affect the area law at large loops, which is responsible for quark confinement.

Remark 2.2. The parameter κ is not determined by the chain of MM equations, nor by the initial value at the vanishing loop $W[0] = 1$ (as $S[0] = 0$). The boundary condition $W[\infty] = 0$ only requires $\kappa \geq 0$. Therefore, this parameter is a free nonperturbative parameter, similar to the vacuum expectation value $\langle \text{tr} F_{\mu\nu}^2 \rangle$. The MM equations reflect the equations of motion of QCD, but not the property of the vacuum, so this ambiguity in the solutions of the equations of motion is inevitable: one must add some information regarding the properties of the gluon vacuum state. Later in this paper, we relate this parameter κ to the slope of the Regge trajectories, which tells us that it is positive in the physical vacuum and has the same dimension as

$\Lambda_{QCD} \sim M^2$. Ideally, in complete theory, one would have to relate it directly to Λ_{QCD} times a universal dimensionless factor. This important task exceeds the scope of the present paper.

3. Hodge -dual minimal surface

Now, we are going to define the solvable functional $S[C]$ satisfying both the duality and additivity. We are following the general construction from [4], but here we correct an error made in that paper: we only need three components of the quaternionic field X_μ , not four¹.

3.1. The surface

We define the surface coordinates $X_\mu^i(\xi)$ (for $\xi = (\xi_1, \xi_2)$, $i = 1, 2, 3$ and $\mu = 1, 2, 3, 4$) Our surface area is defined as

$$S_\chi[C] = \int_{\mathcal{D}} d^2\xi \sqrt{\Sigma_{\mu\nu}^2/2}; \quad (3.1)$$

The area element is defined as

$$\Sigma_{\mu\nu} = \epsilon_{ab} \partial_a X_\mu^i \partial_b X_\nu^i; \quad (3.2)$$

The Hodge chirality $\chi = \pm 1$ enters through the boundary conditions

$$X_\mu^i(\partial\mathcal{D}) = \eta_{\mu\nu}^{i,j} C_\nu; \quad (3.3)$$

Here $\eta_{\mu\nu}^{i,j}$ are 't Hooft's matrices corresponding to Hodge duality $\chi = \pm 1$

$$\eta_{\mu\nu}^{i,j} = \delta_{i\mu} \delta_{j\nu} - \delta_{i\nu} \delta_{j\mu} + \chi \epsilon_{i\mu\nu 4}; \quad (3.4)$$

The coordinate functions $X_\mu^a(\xi)$ satisfy the general Euler-Lagrange equations for the area density $\mathcal{L} = \sqrt{\Sigma^2}/2$:

$$[\text{E-L Equations}]_\mu^a = \epsilon_{lm} \partial_l \left(\frac{\Sigma_{\mu\nu} \partial_m X_\nu^a}{\sqrt{\Sigma^2}} \right) = 0. \quad (3.5)$$

Assuming the bulk variation vanishes by the Euler-Lagrange equations, we use Stokes theorem and get the boundary term

$$\delta S = 2 \int d\theta \frac{\delta X_\mu^i \Sigma_{\mu\nu} \partial_\theta X_\nu^i}{\sqrt{\Sigma^2}} \quad (3.6)$$

Substituting the boundary conditions for δX , $\partial_\theta X$ and summing over $a = 1, 2, 3$ we find

$$\delta S = -2 \int d\theta \frac{\delta C_\mu \Sigma_{\mu\nu} \partial_\theta C_\nu}{\sqrt{\Sigma^2}} \quad (3.7)$$

Therefore, the Hodge duality of the area element Σ with these boundary conditions for generic field

¹the fourth component was worse than unnecessary, it canceled the correct area derivative, produced by the first three components. In the general proofs in that paper, this cancellation was overlooked. The intended results are restored by dropping the fourth component.

$X_\mu^a(z, \bar{z})$ leads to the same Hodge duality of the area derivative.

This self-duality of area derivative makes our Hodge-dual minimal area a zero mode of the loop diffusion operator, leading to the solution of the MM loop equations [2, 3], as we argued in the next section.

Note that this area functional is invariant under the reparametrizations of the boundary loop $\delta_{\text{param}} C_\mu(s) = \epsilon(s) \partial_s C_\mu(s)$

$$\delta_{\text{param}} S = -2 \int ds \epsilon(s) \frac{\partial_s C_\mu \Sigma_{\mu\nu} \partial_s C_\nu}{\sqrt{\Sigma^2}} = 0 \quad (3.8)$$

by the skew symmetry of $\Sigma_{\mu\nu}$.

The Hodge-dual area is defined as a minimum of this functional under an extra duality constraint

$$*\Sigma_{\mu\nu} \equiv \frac{1}{2} \epsilon_{\mu\nu\alpha\beta} \Sigma_{\alpha\beta} = \chi \Sigma_{\mu\nu} \quad (3.9)$$

In the previous paper [4], we found exact solutions for the special case of a planar bounding loop and proved two inequalities. Unfortunately, four components of X field instead of three were erroneously used in that work. In this paper, we find a complete solution for the Hodge-dual surface, superseding the results of previous work and correcting these errors.

3.2. The Holomorphic Ansatz

We resolve the duality constraint using the following holomorphic Ansatz:

$$X_\mu^i = \eta_{\mu\nu}^{i,j} Y_\nu \quad (3.10)$$

$$Y_\mu = f_\mu(z) + \bar{f}_\mu(\bar{z}); \quad (3.11)$$

$$z = \xi_1 + i\xi_2; \quad (3.12)$$

$$\Sigma_{\mu\nu} = 2i(F_{\mu\nu} + \chi * F_{\mu\nu}); \quad (3.13)$$

$$F_{\mu\nu} = f'_\mu \bar{f}'_\nu - \bar{f}'_\mu f'_\nu; \quad (3.14)$$

Geometrically, this is a projection from $\mathbb{R}^3 \otimes \mathbb{R}^4$ to \mathbb{C}^4 . The boundary conditions for the Hodge-dual surface become a conventional boundary condition for the Dirichlet problem

$$2\Re f_\mu(e^{i\theta}) = C_\mu(\theta) \quad (3.15)$$

So, we have a surface in four dimensional complex space $f \in \mathbb{C}^4$. Our surface area (3.1) reduces to the induced metric in this space

$$\Sigma_{\mu\nu} = 2i(F_{\mu\nu} + \chi * F_{\mu\nu}); \quad (3.16)$$

$$F_{\mu\nu} = f'_\mu \bar{f}'_\nu - \bar{f}'_\mu f'_\nu; \quad (3.17)$$

$$\sqrt{\Sigma_{\mu\nu}^2/2} = 2\sqrt{2} \sqrt{-\det g}; \quad (3.18)$$

$$g_{ab} = \partial_{z_a} Y_\mu \partial_{z_b} Y_\mu; \quad z_a, z_b = (z, \bar{z}) \quad (3.19)$$

This area element is Hodge-dual

$$*\Sigma_{\mu\nu} = \chi \Sigma_{\mu\nu} \quad (3.20)$$

for arbitrary functions $f_\mu(z)$.

This duality condition, as argued above, together with the above boundary conditions, provides the self-duality of the area derivative of the minimal area. The self-duality of the area derivative follows from the general formula for variation of the surface $X_\mu^a(\xi)$ with area (3.1), projected on the holomorphic Ansatz.

3.3. The Virasoro Constraint and Uniformization

We further impose a Virasoro constraint on the holomorphic maps derivatives

$$f'_\mu(z)^2 = 0 \quad (3.21)$$

The imposition of the null constraint $(f')^2 = 0$ is not an approximation but a rigorous gauge fixing procedure rooted in the geometric symmetries of the problem.

The physical starting point is the geometric Area functional, $S = \int \sqrt{-\det g} d^2z$, which possesses full reparametrization invariance under general diffeomorphisms $z \rightarrow w(z, \bar{z})$. This infinite symmetry group allows us to choose a specific coordinate system on the world-sheet without altering physical results.

We choose to work in **isothermal (conformal) coordinates**, where the induced metric is diagonal:

$$ds^2 = \rho(z, \bar{z}) dz d\bar{z} \implies g_{zz} = \partial_z Y \cdot \partial_z Y = 0 \quad (3.22)$$

For our specific ansatz (3.10), the metric component g_{zz} is explicitly proportional to the square of the holomorphic derivative:

$$g_{zz} = (f'_\mu)^2 \quad (3.23)$$

Thus, the geometric condition of conformal gauge fixing $g_{zz} = 0$ is algebraically equivalent to the null constraint $(f')^2 = 0$.

The existence of such a coordinate system for any surface topology is guaranteed by the **Uniformization Theorem** [6]. This theorem ensures that we are always free to set $(f')^2 = 0$ by a suitable diffeomorphism. In this gauge, the non-linear geometric area density simplifies exactly to the quadratic Lagrangian:

$$\mathcal{L} = \sqrt{-\det g} = \sqrt{(g_{z\bar{z}})^2 - |g_{zz}|^2} \xrightarrow{(f')^2=0} g_{z\bar{z}} \propto |f'|^2 \quad (3.24)$$

This reduction allows us to describe the Minimal Surface using the linear Laplace equation for f_μ , subject to the Virasoro constraint. To summarize, we have found that

$$S_\chi[C] = 2\sqrt{2} \int_D |f'(z)|^2 d^2z; \quad (3.25)$$

$$\frac{\delta S_\chi[C]}{\delta \sigma_{\mu\nu}} = 2 \frac{\Sigma_{\mu\nu}}{\sqrt{\Sigma_{\mu\nu}^2}}; \quad (3.26)$$

$$\Sigma_{\mu\nu} = 2(F_{\mu\nu} + \chi * F_{\mu\nu}); \quad (3.27)$$

$$F_{\mu\nu} = i(f'_\mu \bar{f}'_\nu - \bar{f}'_\mu f'_\nu); \quad (3.28)$$

The solution of the linear boundary problem (3.15) for a holomorphic vector function is given by the Hilbert transform

$$f_\mu = \frac{1}{2}(1 + i\mathcal{H})C_\mu \quad (3.29)$$

In terms of the Taylor coefficients

$$f_\mu(z) = \sum_{n>0} z^n C_{\mu,n}; \quad (3.30)$$

$$C_\mu(\theta) = \sum_{n=-\infty}^{\infty} e^{in\theta} C_{\mu,n} \quad (3.31)$$

In presence of the Virasoro constraint (3.21), the problem becomes a challenging one, and it was investigated over the last centuries by great mathematicians, starting with Riemann and Hilbert. We give a brief summary of modern state of this theory in [Appendix A](#).

However, for the solution of the quark confinement problem, this general theory can be bypassed, which leads to solvable equations for relativistic quarks in the presence of a confining force coming from our minimal surface. This new theory will be described in subsequent sections.

3.4. Comparing Hodge-dual and the conventional minimal surface

The conventional minimal surface in \mathbb{R}^4 is described by a similar parametric equation $X_\mu(\xi)$ with one instead of three internal components of the X_μ^a field. The corresponding functional:

$$S_{\text{Eucl}}[C] = \int_D d^2\xi \sqrt{\Sigma_{\mu\nu}^2/2}; \quad (3.32)$$

$$\Sigma_{\mu\nu} = \epsilon_{ab} \partial_a X_\mu \partial_b X_\nu; \quad (3.33)$$

$$X_\mu(\partial\mathcal{D}) = C_\mu; \quad (3.34)$$

leads to the similar first variation and area derivative

$$\delta S = 2 \int d\theta \frac{\delta X_\mu \Sigma_{\mu\nu} \partial_\theta X_\nu}{\sqrt{\Sigma^2}}; \quad (3.35)$$

$$\frac{\delta S}{\delta \sigma_{\mu\nu}} = 2 \frac{\Sigma_{\mu\nu}}{\sqrt{\Sigma^2}} \quad (3.36)$$

with the important distinction that the area element $\Sigma_{\mu\nu}$ is neither self-dual nor anti-dual in this case.

This difference is not visible at the level of the minimal value of the area. The holomorphic solution in the \mathbb{R}^4 case, with the same Virasoro constraint for conformal metric

$$X_\mu = f_\nu(z) + \bar{f}_\mu(\bar{z}); \quad (3.37)$$

$$(f'_\mu)^2 = 0; \quad (3.38)$$

$$\Sigma_{\mu\nu} = 2i(f'_\mu \bar{f}'_\nu - f'_\nu \bar{f}'_\mu) \quad (3.39)$$

leads to the Dirichlet functional for the minimal \mathbb{R}^4 area

$$S_{\text{Eucl}}[C] = \int_D |f'(z)|^2 d^2z; \quad (3.40)$$

Up to normalization, this is the same functional that we have found for the Hodge dual surface and is independent of Hodge duality χ .

In both cases, this functional equals the net area of conformal maps $f_\mu(z)$ and can be rewritten as the boundary integral.

$$\begin{aligned} S_{\text{Eucl}}[C] &\propto 2 \int d\theta C'_\mu(\theta) \Im f_\mu(\theta) \\ &\propto \int d\theta C'_\mu(\theta) \int d\theta' K(\theta - \theta') C_\mu(\theta') \end{aligned} \quad (3.41)$$

with Hilbert kernel $K(\theta - \theta')$. As observed by Douglas, the Virasoro constraint can be imposed by further minimization of this functional by parametrization of the bounding loop $C(\theta) \Rightarrow C(\phi(\theta))$. The variational equation for this minimization

$$C'_\mu(\theta) \frac{\delta S_{\text{Eucl}}[C]}{\delta C_\mu(\theta)} = 0 \quad (3.42)$$

reduces to

$$\begin{aligned} C'_\mu(\theta) \partial_\theta \Im \partial_\theta f_\mu &\propto \Re \partial_\theta f_\mu \Im \partial_\theta f_\mu \\ &\propto \Im(\partial_\theta f_\mu)^2 \propto \Im(z f'_\mu)^2 = \Im(z^2 (f'_\mu)^2) = 0 \end{aligned} \quad (3.43)$$

which is equivalent to Virasoro constraint at the boundary.

Now we can compute the area derivative of the Dirichlet functional for an arbitrary parameterization of the boundary curve.

The area derivative of this functional, as defined in (2.1) would yield exactly zero, as the second functional derivative is a symmetric tensor proportional to $\delta_{\mu\nu}$. The minimization over parametrizations would not change this fact, as we get zero for arbitrary parametrization. The area derivative of the minimal value of the Douglas-Dirichlet functional corresponds to the area derivative of this functional, taken at the optimal parametrization. This area derivative would, therefore, yield zero.

We conclude that the area derivative of the holomorphic functional yields zero, contradicting exact computations for the full area functional.

So, the area derivative, for some reason, involves more than just the minimal value of the area considered as a functional of its boundary. This paradox is discussed in the next section.

3.5. The hidden variables of the minimal surface

The apparent paradox is resolved by examining the variational principle in the extended space. The functional $S_\chi[C]$ is defined as the minimum of the area functional for a surface $X_\mu^a \in \mathbb{R}^3 \otimes \mathbb{R}^4$. Crucially, the boundary of this extended surface is rigidly locked to the physical loop C_μ via the chiral 't Hooft symbols:

$$X_\mu^a \Big|_\partial = \eta_{\mu\nu}^{\chi, a} C_\nu \quad (3.44)$$

When we compute the area derivative, we vary the physical loop C_μ in standard 4D space. However,

due to the boundary coupling, this 4D variation **induces** a specific variation of the surface in the 12-dimensional embedding space. We are probing the shape of this 12-dimensional surface in the vicinity of its 4-dimensional edge.

By the Envelope Theorem (or the principle of stationary action), the variation of the minimal value with respect to the boundary parameters is determined solely by the boundary terms, as the bulk Euler-Lagrange variations vanish. Thus:

$$\delta S_\chi = \oint d\theta \frac{\delta \mathcal{L}}{\delta (\partial_\theta X_\mu^a)} \delta X_\mu^a = \oint d\theta \Pi_\mu^a (\eta_{\mu\nu}^{\chi, a} \delta C_\nu) \quad (3.45)$$

While the scalar minimal value of the action (the energy) is invariant under the isometric embedding η , the conjugate momentum Π_μ^a and the boundary coupling η carry the chiral index. The first variation δS vanishes at the minimal surface, but the area derivative involves the second variation, related to variation of this conjugate momentum by C' . So to say, we are measuring the elasticity of the spring, which pulls the surface in 12D to its minimal shape. This minimal shape, does not depend on chirality but the elasticity tensor does.

The same arguments explain the difference between the area derivative of the ordinary Nambu-Goto area functional and the Dirichlet functional. The area derivatives uses the Hessian of the functional at the minimum, which is different for the full functional and the holomorphic projection, minimizing this full functional. This difference is responsible for the nonzero value of area derivative for the Nambu-Goto area functional

The analogy would be the computation of the hessian of the function of several variables at the extremal set, where the gradient of this function vanishes. Neither the extremal value of the function, nor this vanishing gradient depend on some hidden parameters, but the hessian does.

Remark 3.1 (Toy example: same minimum value, different second variations). *Let*

$$F_a(x, y) = (y - ax)^2 + x^2 \quad (a \in \mathbb{R}).$$

Then $y_(x) = ax$ minimizes in y and the minimized value is*

$$g_a(x) := \min_y F_a(x, y) = F_a(x, ax) = x^2$$

independent of a . Yet the x -Hessian of the full functional on the minimizing locus depends on a :

$$\left. \frac{\partial^2 F_a}{\partial x^2} \right|_{y=ax} = 2(1 + a^2) \neq g_a''(x) = 2.$$

3.6. Symmetrization of the area by parity

The extremal value

$$S_\chi[C] := \min_X S_\chi[X; C]$$

is χ -independent, but the loop-space area derivative—defined as the discontinuity of the second variation and evaluated on the χ -dependent stationary surface in the extended space—retains χ -dependence through the boundary locking. This chirality independence of the minimal value is manifest in the Holomorphic Ansatz: neither the Dirichlet functional (3.26), nor the Virasoro constraint (3.21), nor the boundary condition (3.15) depend on χ . This common minimal value corresponds to a particular solution of the Plateau problem—the one which is additive over disconnected parts of the loop, including the parts arising at self-intersections. In the confining factor below, we preserve the parity of QCD by using a symmetric combination:

$$S[C] = \frac{1}{2}(S_+[C] + S_-[C]) \quad (3.46)$$

Its value equals the common value of these two functionals, but each term represents a different zero mode of the loop operator \mathcal{L} in (2.3), distinguished by Hodge duality $\chi = \pm 1$. The area derivative of the symmetrized area (3.46) is proportional to that of the Nambu-Goto string. By summing the self-dual and anti-self-dual projections:

$$\begin{aligned} \frac{\delta S}{\delta \sigma} &= \frac{1}{2} \left(2 \frac{F + *F}{|F + *F|} + 2 \frac{F - *F}{|F - *F|} \right) \\ &= \frac{2F}{\sqrt{F^2 + (*F)^2}} = \frac{F \sqrt{2}}{|F|} \end{aligned}$$

Note that for the standard Nambu-Goto string, this factor would simply be $\frac{2F}{|F|}$. The difference is a factor of $\sqrt{2}$.

One may then ask: why do we need the Hodge-dual surface at all? If the area derivative of the symmetrized Hodge-dual surface is equivalent (up to normalization) to that of the Nambu-Goto string, why not claim the Nambu-Goto string itself solves the loop equation as a zero mode? Direct calculation in [4] shows this is not possible. The area derivative of the conventional minimal area is well-defined, but it does not solve the loop equation: it produces in this equation a singular factor $\frac{\delta}{\delta^2 + \epsilon^2}$, depending on the ratio of the two infinitesimal cut-off parameters involved in the definition of the loop variations. Depending on this ratio, we obtain an arbitrary number between zero and infinity instead of the required zero in the loop equation.

The only way to satisfy the loop equation is to return to the symmetric sum of the *full functionals* (3.46), apply the area derivative to each term, and utilize the crucial identity that the sum of the derivatives relates to the difference of their duals:

$$\begin{aligned} \frac{\delta S}{\delta \sigma} &= * \frac{\delta S_+}{\delta \sigma} - * \frac{\delta S_-}{\delta \sigma}, \\ \frac{\delta S_\chi}{\delta \sigma} &\propto (F + \chi * F) / \sqrt{F^2}; \\ F_{\mu\nu} &= \Im f_\mu \bar{f}_\nu \end{aligned}$$

We recall that each of these individual area derivatives $\frac{\delta S_\chi}{\delta \sigma}$ is the antisymmetric tensor part of the second derivative $\frac{\delta^2 S_\pm}{\delta C'_\mu(\theta-) \delta C'_\nu(\theta+)}$. We can then apply the Bianchi identity (2.5) to each term independently to satisfy the loop equation. At the technical level, the dot derivative $\frac{\delta}{\delta C'_\mu}$ when applied to $(F_{\mu\nu} + \chi * F_{\mu\nu}) / \sqrt{F^2}$ yields this singular factor $\frac{\delta}{\delta^2 + \epsilon^2} \dot{C}'_\nu$, but when the area derivative is represented exactly as the extremal value of $\chi * \frac{\delta^2 S_\chi}{\delta C'_\mu(\theta-) \delta C'_\nu(\theta+)}$, the same dot derivative $\frac{\delta}{\delta C'_\mu}$, taken before projecting on the holomorphic minimizer, yields zero by Bianchi identity.

In other words, the value of the area derivative of the symmetric combination $S_+ + S_-$ is not sufficient to compute the third derivative $\frac{\delta}{\delta C'}$ involved in the loop equation: one must retain the full functional definitions of the components S_\pm . The Bianchi identity allows us to bypass the laborious direct computation of this third functional derivative by exploiting the Hodge dualities of the two area derivatives. However, were we to perform this direct computation without invoking the Bianchi identity—retaining the full structure of S_\pm —we would find that the net contribution to the loop equation vanishes regardless. The singularities that plague the Nambu-Goto string, as well as the regular terms, must cancel exactly between the two chiral sectors to satisfy the Bianchi identity.

As an example of such a cancelation, one could consider a similar cancelation of Feynman diagrams in the expectations of $\hat{P}[D_\mu, *F_{\mu\nu}] \exp(\int Adx)$. With dimensional regularization, these diagrams cancel including regular and singular parts (poles in $\epsilon = 4 - d$).

3.7. Planar Loop Solution

We consider the specific ansatz for a planar loop where the derivative of the coordinate vector, $f'_\mu(\xi)$, is defined by a single scalar holomorphic function $w'(\xi)$ multiplied by a constant isotropic vector:

$$f'_\mu(\xi) = w'(\xi) \begin{pmatrix} \frac{1}{\sqrt{2}} \\ \frac{-i}{\sqrt{2}} \\ 0 \\ 0 \end{pmatrix}_\mu \quad (3.47)$$

3.8. Verification of Null Condition

The null condition $(f'(\xi))^2 = 0$ is satisfied identically due to the vector structure:

$$\sum_{\mu=1}^4 f'_\mu f'_\mu = (w'(\xi))^2 \frac{1^2 + (-i)^2 + 0^2 + 0^2}{2} = 0 \quad (3.48)$$

3.9. Coordinate Integration

The spacetime coordinates $X_\mu^a(\xi)$ are recovered by integrating the holomorphic derivatives. Assuming the physical coordinates are the real part of the holomorphic trajectory $X_\mu^a(\xi) = 2\eta_{\mu\nu}^{a,\chi}\Re f_\nu(z)$:

$$\Re f_1(z) = \Re[w(z)] \quad (3.49)$$

$$\Re f_2(z) = \Re[-iw(z)] = \Im[w(z)] \quad (3.50)$$

$$\Re f_3(z) = 0 \quad (3.51)$$

$$\Re f_4(z) = 0 \quad (3.52)$$

3.10. Resulting Geometry

This solution represents (up to rotation with η^a matrices) a general conformal mapping from the parameter domain ξ directly to the physical plane (X_1, X_2) , with trivial coordinates in the transverse dimensions X_3, X_4 . The function $w(\xi)$ completely determines the shape of the planar loop. This planar solution matches the one found in [4] for planar loop.

Verification of the Loop Equation. For this planar solution, we can explicitly verify the zero-mode condition. The area derivative for the planar ansatz reduces to the simple algebraic form $\delta S_\chi / \delta \sigma_{\mu\nu} \propto (F_{\mu\nu} + \chi * F_{\mu\nu}) / \sqrt{F^2}$ which is manifestly self-dual. Therefore, the condition $*\frac{\delta S_\chi}{\delta \sigma} = \chi \frac{\delta S_\chi}{\delta \sigma}$ holds pointwise. By the Bianchi identity (2.5), this implies $\mathcal{L}S[C] \equiv 0$ without reliance on the general loop calculus of Ref [4]. This confirms that the explicit planar solution is indeed an exact zero-mode of the loop operator. This is, however, a rather trivial zero mode, as the normalized tensor $(F_{\mu\nu} + \chi * F_{\mu\nu}) / \sqrt{F^2} \propto \eta_{\mu\nu}^{3,\chi}$ is a universal constant tensor, with vanishing functional derivative.

4. Topological Stability and General Variational Principle

4.1. Stationarity and Boundary Variation

Let C be a self-intersecting loop. The Hodge surface minimization problem admits an **additive solution** Σ_{add} which is a stationary point (local minimum) of the geometric Area functional $S[X]$ defined on the extended space of maps $X : \mathcal{D} \rightarrow \mathbb{R}^3 \otimes \mathbb{R}^4$.

Because Σ_{add} is a stationary point, the coordinate functions $X_\mu^a(u, v)$ satisfy the general Euler-Lagrange equations for the area density $\mathcal{L} = \sqrt{\Sigma^2}/2$. This condition ensures that for *any* variation δX_μ^a in the wider functional space (not limited to holomorphic functions), the bulk contribution to the variation of the action vanishes:

$$\delta_{bulk} S = - \int_D d^2 \xi \delta X_\mu^a [\text{E-L Equations}]_\mu^a. \quad (4.1)$$

Consequently, the total variation of the area functional reduces exactly to the boundary flux term derived in (3.6). This validates the computation of the area derivative and subsequent proof of its Hodge-duality for arbitrary loop as long as the surface $X_\mu^a \in \mathbb{R}^3 \otimes \mathbb{R}^4$ minimizes the area functional (3.1).

The existence of the additive minimal solution is guaranteed by the results of [7] and [8], who established that the disconnected solution minimizes the functional for separated or touching boundaries. Since the surface is an extremum in the full functional space, the bulk variation vanishes identically by the principle of stationary action.

Remark 4.1 (Stability of the Goldschmidt Solution). *While a connected minimal surface (global minimum) may exist, the QCD Loop Equation requires the additive Goldschmidt solution to satisfy the factorization condition $S[C_1 \cdot C_2] = S[C_1] + S[C_2]$. The topological barrier proven by [9] ensures that this additive solution is a local minimum, which is all we need for the proof of Hodge-duality.*

Remark 4.2. *The continuity of the transition between a single loop with an infinitesimal neck and two touching loops (the self-intersecting limit) is mathematically grounded in the Bridge Principle for stable minimal surfaces [10]. This principle establishes that given two stable minimal surfaces bounded by curves C_1 and C_2 , one can construct a connected minimal surface bounded by a single loop formed by joining C_1 and C_2 with a thin “bridge” of width ϵ . As $\epsilon \rightarrow 0$, this connected surface converges smoothly (in the varifold sense) to the union of the original surfaces. Consequently, the Goldschmidt solution we utilize—which effectively treats the area as additive, $\mathcal{A}(C_1 \cup C_2) = \mathcal{A}(C_1) + \mathcal{A}(C_2)$ —represents the correct continuous limit of the loop equation dynamics, avoiding the discontinuous jumps associated with the global minimization of the Plateau problem (such as the catenoid collapse). This ensures that the loop derivative remains well-defined across topology changes. Specifically, because the convergence is smooth in the varifold sense, the functional derivatives required for the loop equation (which probe the surface near the loop C) are continuous limits of the derivatives of the connected surface, justifying the application of the differential loop calculus to the additive Goldschmidt functional.*

We assume (or conjecture, supported by [7, 8, 10]) that the Goldschmidt/local-minimum branch defines a continuous additive functional on immersed loops with transverse self-intersections, and that the loop-space area derivative exists almost everywhere along each branch. Under this assumption, Theorem 2.1 applies.

5. Confinement theorem

Now, we can summarize the arguments of the previous section in a theorem.

Theorem 5.1 (Confinement area law). *The common minimal value of self-dual (and anti-dual) area $S_\chi[C]$ for any loop without self-intersections is equal to the ordinary euclidean minimal area bounded by the same loop*

$$S_\chi[C] = 2\sqrt{2}\mathcal{A}_{\text{Plateau}}[C] \quad (5.1)$$

At self-intersections or for several disconnected closed components of the loop the area is additive over closed parts, unlike the euclidean minimal area which may change topology for a smaller area.

Proof. The minimal value of Self-Dual Area S_χ is given by the Dirichlet integral (3.26) with boundary conditions

$$2\Re f_\mu(e^{i\theta}) = C_\mu(\theta)$$

under the Virasoro constraint (3.21). These are exactly the conditions of the classical Plateau problem. Therefore, every local minimum of our problem is also the local minimum of the Plateau problem. The difference between solutions could arise in case of self-intersecting loop when there could be several local minima. Our solution selects the one that is additive over the closed parts of the loop (the Goldschmidt solution), whereas the Plateau problem selects the global minimum, which could be topologically different (say, a cylindrical surface bounded by both parts of the loop). According to the theorems [8, 7, 9], such a disconnected, locally minimal surface always exist. \square

Remark 5.1. *The equality of the areas $S_\pm[C]$ only holds for the minimal values. These areas are different as functionals, which leads to a difference in the second order functional derivatives at the minimum. As a result, the area functional $S_\chi[C]$ has the area derivatives with Hodge duality $\chi = \pm 1$ despite having common minimal value. This phenomenon was discussed in section 3.5 above.*

Remark 5.2. (Distinction from String Theory and Lattice Strong Coupling). *Unlike the lattice QCD strong-coupling expansion, there are no intrinsic “worldsheet” modes in our rigid minimal surface to generate daughter trajectories. While strong-coupling expansions in lattice gauge theory do involve sums over tessellated surfaces, these are essentially lattice artifacts that do not survive the continuum limit. It is well known that a sum over random surfaces does not exist in the 4D continuum theory due to conformal anomalies (which lead to the branched polymer instability); these anomalies are often undetectable in coarse lattice simulations. Consequently, using the lattice strong-coupling phase as a guide for the continuum theory*

is misleading, as it fails to respect fundamental continuum symmetries—specifically the conformal anomalies and the Hodge duality required for the mechanism described here. Our solution operates in the continuum limit where these constraints enforce a unique, rigid minimal surface rather than a sum over fluctuating surfaces.

Remark 5.3. *We must also specify the definition of the perturbative factor $W_{\text{pert}}[C]$ in the Wilson loop. It is uniquely defined as an asymptotic expansion generated by iterating the MM equations [2, 3], starting from $W = 1$. However, the summation of this asymptotic series is not unique beyond the perturbation expansion, which proceeds in powers of the running coupling constant $\lambda_{\text{eff}}[C] \sim 1/\log(\Lambda_{\text{QCD}}|C|)$. Consequently, non-perturbative terms, such as our dressing factor, appear at double-exponential order:*

$$\exp\left(-\exp\left(\frac{\text{const}}{\lambda_{\text{eff}}[C]}\right)\right)$$

The ambiguity associated with adding the dressing factor with an arbitrary parameter κ corresponds to this inherent ambiguity in perturbative QCD. To be specific, we may define $W_{\text{pert}}[C]$ as the Borel sum of the gluon diagrams in the perturbative expansion. The ambiguity of this Borel sum matches the freedom in the choice of κ . We must acknowledge that our theory of confinement remains incomplete until a unique definition of $W_{\text{pert}}[C]$ is established, along with the precise relationship between κ and the QCD mass scale Λ_{QCD} .

Subject to these caveats, we have established a precise correspondence between QCD and the area law. As demonstrated in the following section, this framework yields the standard rising Regge trajectories while avoiding the typical inconsistencies associated with string theory in four dimensions. Our approach relies solely on minimal surfaces—a classical and well-defined subject in modern geometry. While the mathematical theory of minimal surfaces as solutions to the Plateau problem is extensive (briefly summarized in Appendix A), it generally does not provide explicit analytic solutions for an arbitrary loop C .

Fortunately, the main application of our minimal surface – the rising meson spectrum in QCD – does not require such a general solution. The relevant loops in this case, as we shall see below, simplify, allowing for the analytic solution for the minimal surface and directly leading to linear Regge trajectories..

6. Effective Lagrangian and Regge Trajectories

In this section, we derive the effective Lagrangian for the quark-antiquark pair connected by the con-

fining flux. We describe the confining geometry using the Minkowski Helicoid. It is important to clarify the theoretical justification for this choice. The Helicoid (the ruled surface, made of the rotating stick, Fig. 1) is well-known (see Appendix A) as a minimal surface in Euclidean space (where it minimizes area).

Technically, our computation goes along the same lines as that in the classical string theory textbooks [11, 12]. We repeat these steps here to demonstrate that the dynamics of the string as a physical body do not affect the Regge trajectory in the WKB approximation at large angular momenta, when the masses grow. This WKB method applies to our "holographic string" in the same way as it applies to the physical string considered in these textbooks. The crucial difference is that in our theory we do not have vibrational degrees of freedom to add to the spectrum (and create instabilities in 4D).

The conventional string theory uses the minimal surface as the leading order of the WKB approximation and is forced to add the contribution of the fluctuations of the string shape. In our theory, this is a WKB approximation for the rotation of a pair of quarks under a static force induced by the gluon vacuum.

6.1. The Minkowski Helicoid

The Minkowski Helicoid is parameterized by time $\tau \in [0, T]$ and radius $r \in [-R, R]$, see [13]. The time T tends to infinity in the end.

$$X(\tau, r) = (r \cos \omega\tau, r \sin \omega\tau, 0, \tau) \quad (6.1)$$

The induced Minkowski metric is $g_{ab} = \text{diag}(1 - \omega^2 r^2, 1)$.

In Minkowski space we are not seeking to minimize the area in the geometric sense, as the area functional is not positive definite and the minimization problem is distinct. Instead, our criterion is algebraic: we require a solution to the Loop Equations for the Wilson loop. This demands the self-duality of the area derivative and the additivity of the area functional. We utilize the fact that the Euclidean Helicoid is a minimal surface for arbitrary angular velocity ω . We obtain the Minkowski Helicoid via a double Wick rotation:

$$x_4 \rightarrow it, \quad \omega_E \rightarrow -i\omega. \quad (6.2)$$

Under this transformation, the argument of the trigonometric functions in the coordinate parametrization becomes real ($\omega_E x_4 \rightarrow \omega t$), mapping the Euclidean Helicoid to a real surface in Minkowski space. Crucially, the condition that $S[C]$ is a zero mode of the Loop Equation depends on algebraic identities (self-duality of the area derivative and additivity). By the Identity Theorem, these analytic relations, established for

the Euclidean minimal surface, must hold for its analytic continuation into Minkowski space. Thus, the Minkowski Helicoid remains a valid solution to the QCD Loop Equation, bypassing the ill-posed variational problem of minimizing area in a space with indefinite metric. Another important point

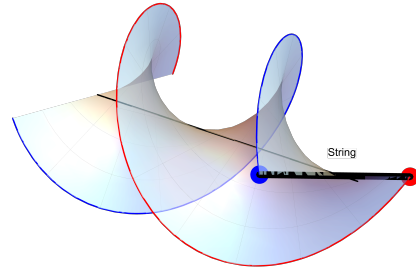


Figure 1: The helicoid spanned by rotating $\bar{q}q$ pair connected by a rigid stick (string). This minimal surface bounded by a double helix, was discovered by Meusnier in 1785.

is that the Helicoid boundary loop (double helix) is **infinitely smooth**, lacking any cusps or self-intersections. This means that no UV divergent renormalization factors in the perturbative Wilson loop factor $W_{\text{pert}}[C]$ could potentially affect our computation of the meson Regge trajectory.

6.2. Semiclassical Motivation: Twisted Boundary Conditions

Before solving the spectral equation, we justify the choice of the Helicoid geometry from the perspective of the semiclassical quark path integral.

Consider the Green's function for a meson composed of scalar quarks with mass m . In the quenched approximation, the effective Minkowski action involves a sum over quark trajectories C , weighted by the quark mass term and the area of the confining minimal surface Σ bounded by C . Neglecting the perturbative factor² in the Wilson loop at large loops, relevant to our WKB approximation:

$$\mathcal{Z} \sim \int \mathcal{D}C \exp \left(-im \oint_C ds - i\sigma S_{\text{Mink}}[\Sigma_C] \right) \quad (6.3)$$

To extract the spectrum of states with angular momentum J , we impose *twisted boundary conditions*. We require the quark positions at time $t = T$ to be a rotation of their positions at $t = 0$ by an angle $\Theta = \omega T$ in the rotation plane xy :

$$(x + iy)(T) = e^{i\omega T} (x + iy)(0) \quad (6.4)$$

The angular momentum J arises as the thermodynamic conjugate to the twist frequency ω .

²the perimeter renormalization terms in that factor we include in the physical quark mass.

The ground state of this system is determined by the saddle point of the effective action. This requires the simultaneous minimization of the boundary length (quark term) and the surface area (gluon term).

- The minimization of the boundary length for a rotating particle yields a helical trajectory in Minkowski spacetime.
- The minimal surface spanning two twisted helical boundaries is the **Helicoid**.

Thus, the Helicoid is not merely an ansatz; it is the unique geometric solution mandated by the kinematics of angular momentum in the semiclassical limit. The balance between the surface tension σ (pulling the quarks inward) and the centrifugal barrier (pushing the twisted trajectories outward) determines the physical radius of the meson.

6.3. Effective Lagrangean

We construct the effective Lagrangian L by combining the bulk contribution from the Helicoid area (coming from our confining factor) with the worldline terms for the massive quarks. The confining factor introduces an effective Minkowski area term. We interpret the phase factor for quark propagation as an effective action, adding the worldline terms $2m \int ds$. The total Lagrangian is:

$$L = L_{\text{helicoid}} + L_{\text{quarks}} \quad (6.5)$$

The Helicoid contribution, calculated as the area integral in Minkowski space for a ruled surface with angular velocity ω and radius $R = v/\omega$, is:

$$\begin{aligned} L_{\text{helicoid}} &= -\sigma \int_{-R}^R dr \sqrt{1 - \omega^2 r^2} \\ &= -\frac{\sigma}{\omega} \left(v \sqrt{1 - v^2} + \arcsin v \right) \end{aligned} \quad (6.6)$$

Here σ is the physical string tension, related to the parameter κ in the confining factor $\exp(-\kappa S[C])$ by the relation $\sigma = 2\sqrt{2}\kappa$, which accounts for the normalization of the Hodge-dual area functional. Adding the particle term $-2m\sqrt{1-v^2}$ as specified for the massive endpoints, the total effective Lagrangian becomes:

$$L(v, \omega) = -\frac{\sigma}{\omega} \left(v \sqrt{1 - v^2} + \arcsin v \right) - 2m \sqrt{1 - v^2} \quad (6.7)$$

It is worth noting, that this mass term is proportional to the perimeter of the loop in Minkowski space. Therefore, the potential perturbative terms proportional to the loop perimeter, are included in this physical quark mass m . We are assuming that this physical mass (the bare quark mass plus perturbative corrections) adds up to a finite renormalized mass m , which, as the experiment tells

us, is much smaller than the QCD mass scale, so that $m^2 \ll \kappa$.

We proceed to compute the conserved quantities via the Legendre transform. The angular momentum J is the conjugate momentum to the rotation frequency:

$$J = \frac{\partial L}{\partial \omega} \quad (6.8)$$

Taking into account that v depends on ω via the fixed radial extent ($v = \omega R$), the differentiation yields:

$$J = \frac{\sigma}{\omega^2} (\arcsin v - v \sqrt{1 - v^2}) + \frac{2mv^2}{\omega \sqrt{1 - v^2}} \quad (6.9)$$

The Energy E is defined by the Hamiltonian $E = \omega J - L$. Substituting the expressions for J and L and simplifying the algebra, we obtain:

$$E = \frac{2\sigma}{\omega} \arcsin v + \frac{2m}{\sqrt{1 - v^2}} \quad (6.10)$$

6.4. Balance of quark forces and boundary condition

The relationship between the endpoint velocity v and the string length R is not arbitrary; it is determined by the balance of forces at the string endpoint, which depend on the quark mass m . We derive this boundary condition by minimizing the action with respect to the geometric radius R of the loop, keeping the angular velocity ω fixed.

Recall that the total Lagrangian L is composed of the bulk integral for the helicoid and the boundary terms for the quarks:

$$L = -2\sigma \int_0^R dr \sqrt{1 - \omega^2 r^2} - 2m \sqrt{1 - \omega^2 R^2} \quad (6.11)$$

The equation of motion for the endpoint radius R is given by the stationarity condition $\frac{\partial L}{\partial R} = 0$. Differentiating the integral using the Leibniz rule yields the tension force, while differentiating the boundary term yields the centrifugal force:

$$\frac{\partial L}{\partial R} = -2\sigma \sqrt{1 - \omega^2 R^2} - 2m \frac{d}{dR} \left(\sqrt{1 - \omega^2 R^2} \right) = 0 \quad (6.12)$$

Substituting $v = \omega R$ and computing the derivative of the mass term:

$$-2\sigma \sqrt{1 - v^2} - 2m \left(\frac{-\omega^2 R}{\sqrt{1 - \omega^2 R^2}} \right) = 0 \quad (6.13)$$

Simplifying the expression, we obtain the exact force balance equation for finite mass:

$$\sigma \sqrt{1 - v^2} = \frac{mv^2}{R \sqrt{1 - v^2}} \implies v^2 = \frac{\sigma R}{\sigma R + m} \quad (6.14)$$

This equation balances the confining string tension (LHS) against the relativistic centrifugal inertia of the quark (RHS).

We now consider the limit $m \rightarrow 0$, and we find the boundary condition

$$v^2 \rightarrow 1 \quad (6.15)$$

Thus, as the quark mass tends to zero, the endpoint velocity v must approach the speed of light ($v \rightarrow 1$).

These equations provide the exact parametric equation for the energy of the classical pair of particles with a given angular momentum and a given radius R . To recover the Regge trajectories, we consider the limit of massless quarks ($m \rightarrow 0$), where the endpoint velocity approaches the speed of light ($v \rightarrow 1$). In this limit, the mass terms vanish, and the system is governed purely by the confining geometry:

$$E \approx \frac{2\sigma \pi}{\omega}, \quad J \approx \frac{\sigma \pi}{\omega^2} \quad (6.16)$$

Eliminating ω between these two relations:

$$J = \frac{\sigma(\pi/2)}{(\pi\sigma/E)^2} \cdot \frac{\pi}{2} \implies J = \frac{E^2}{2\pi\sigma} \quad (6.17)$$

We thus recover the linear Regge trajectory:

$$E^2 = 2\pi\sigma J \quad (6.18)$$

This result confirms that the linear confinement arises directly from the kinematics of the Hodge-dual minimal surface in Minkowski space, without invoking independent string vibrations or ad-hoc constants.

7. Discussion: Comparison with other models of Confinement

A fundamental distinction must be drawn between the geometric solution presented here and the traditional strong coupling expansion in Lattice Gauge Theory (LGT).

In the standard LGT framework, the area law arises in the strong coupling limit ($\beta \rightarrow 0$) through a sum over tessellated surfaces (plaquettes) bounded by the Wilson loop C . While this yields confinement at strong coupling, the analytic continuation of this expansion to the continuum limit ($\beta \rightarrow \infty$) is obstructed by two well-known pathologies: the *Roughening Transition* and the *Branched Polymer instability*.

7.1. The Failure of Surface Sums in the Continuum

As the coupling decreases towards the continuum limit, the surface tension decreases, and the “tessellated surface” undergoes a Roughening Transition [14, 15]. Beyond this point, the transverse fluctuations of the surface diverge, and the simple strong coupling expansion breaks down.

More critically, attempts to formulate the Wilson loop as a sum over random surfaces in continuous 4D Euclidean space encounter a fatal geometric

instability. The entropy of “crumpled” surface configurations overwhelms the Boltzmann weight of the area action. Consequently, the path integral over surfaces is dominated not by smooth 2D sheets, but by **Branched Polymers**—tree-like structures with Hausdorff dimension $d_H = 4$ [16, 17]. This “crumpled phase” is unphysical for a string theory of hadrons.

Furthermore, if one attempts to treat these surfaces as fundamental dynamical strings (e.g., the Polyakov string), the theory suffers from the **Conformal (Liouville) Anomaly**. In $D = 4$, the trace anomaly of the stress tensor leads to a strongly coupled Liouville mode, preventing a consistent quantization of the string without introducing unphysical critical dimensions (such as $D = 26$).

7.2. Stability of the Hodge-Dual Solution

The solution derived in this paper avoids these instabilities entirely because **we do not perform a sum over fluctuating metrics**.

Instead of integrating over a path space of random surfaces, our approach identifies a unique, stable geometric object: the **Hodge-dual minimal surface**. This surface is a classical saddle point of the effective action in loop space, determined rigidly by the boundary loop C and the specific geometry of the Douglas-Gram matrix.

- **No Roughening:** Because the surface is a fixed minimal solution (a “hologram” of the loop) rather than a fluctuating statistical ensemble, it does not undergo a roughening transition.
- **No Branched Polymers:** We do not sum over “crumpled” configurations; we select the analytic minimum.
- **No Liouville Anomaly:** There are no intrinsic string degrees of freedom (2D quantum gravity) to quantize. The surface is an auxiliary geometric construct derived from the gauge field dynamics, not a fundamental quantum string.

The construction requires the summation of the areas of the two Hodge-dual surfaces, S and \tilde{S} . This is dictated by **Parity Conservation**: since the Hodge star operation involves the epsilon tensor, it transforms as a pseudoscalar. Including both surfaces symmetrically ensures the resulting Wilson loop functional is a true scalar, preserving the parity invariance of the strong interaction.

7.3. Distinct from Nambu-Goto String Models

It is crucial to emphasize that this solution does not merely reproduce the standard string model

of confinement. The classic Nambu-Goto string spectrum predicts a tower of “daughter trajectories” arising from the vibrational modes of the flux tube.

In contrast, our solution yields a single linear Regge trajectory. The confining factor $\exp(-\kappa S_{min})$ corresponds to the ground-state static potential $V_0(R)$ between quarks.

We do not deny the existence of excited gluonic levels (often termed “hybrid potentials” or “excited flux tubes” in lattice QCD [18]). However, within our framework, these states are not vibrations of the confining minimal surface itself. The minimal surface is a rigid geometric object fixed by the loop C . Excited states correspond to specific operator insertions or gluonic excitations *on top* of this vacuum background, which would be described by higher-order correlation functions rather than the vacuum expectation value of a single Wilson loop.

Thus, the “missing” daughter trajectories in our result are a feature, not a bug: we separate the universal confining force (the minimal surface) from the specific gluonic excitations, avoiding the unphysical tachyon/Liouville modes inherent to fundamental string theories in $D = 4$.

7.4. Decoupling of Confinement and Correlations

This factorization property provides a crucial insight into the physical nature of the mass gap. Consider the connected correlator for two loops C_1 and C_2 separated by a large distance R :

$$\mathcal{W}_{conn}(C_1, C_2) = \mathcal{W}(C_1 \cup C_2) - \mathcal{W}(C_1)\mathcal{W}(C_2) \quad (7.1)$$

In our framework, the minimal area functional is additive for widely separated loops, $S_{min}[C_1 \cup C_2] = S_{min}[C_1] + S_{min}[C_2]$. Consequently, the non-perturbative confining factor factors out of the correlation completely:

$$\begin{aligned} \mathcal{W}_{conn}(C_1, C_2) &= \exp(-\kappa(S[C_1] + S[C_2])) \\ &[W_{pert}(C_1, C_2) - W_{pert}(C_1)W_{pert}(C_2)] \quad (7.2) \end{aligned}$$

This result implies that the exponential decay of correlations at large distance (the glueball mass gap) is **not** driven by the confining minimal surface. The surface simply provides the background normalization for the quark sources (the confinement mechanism).

Instead, the inter-loop correlation $\exp(-M_{gl}R)$ arises entirely from the term in brackets—the connected part of the perturbative gluon diagrams (“fluctuation factors”). Thus, our solution establishes a clean separation of mechanisms:

1. **Confinement** is a geometric phenomenon governed by the Hodge-dual minimal surface (the area law).
2. **The Mass Gap** (glueballs) and long-range correlations are dynamic phenomena governed by gluon exchange fluctuations (the perturbative pre-factors).

This distinction further explains why our minimal surface remains stable and static: it does not need to vibrate to transmit forces between singlets; those forces are carried by the gluon field itself. The problem of the mass gap in this correlation function is not solved by our confining factor: it requires further nonperturbative insights.

7.5. Our 12D Surface vs. AdS/CFT Holography

Our solution shares the fundamental philosophy of the Holographic Principle: the physical observables (Wilson loops) in 4D spacetime are determined by the geometry of a minimal surface in a higher-dimensional “bulk” space. However, the nature of this target space and the mechanism of holography differ fundamentally from the standard AdS/CFT correspondence.

1. **The Target Space:** In AdS/CFT, the holographic dual is typically a curved 5-dimensional anti-de Sitter space (plus a compact manifold), representing a gravitational theory. In our framework, the “bulk” space is a flat 12-dimensional space, $\mathbb{R}^4 \otimes \mathfrak{su}(2)$, formed by the tensor product of Euclidean spacetime and the canonical $\mathfrak{su}(2)$ subalgebra associated with the self-dual sector (similar to the instanton embedding in arbitrary N_c).
2. **Origin of the Geometry:** We do not postulate a dual gravitational theory. The 12-dimensional geometry arises directly from the non-Abelian structure of the gauge field itself. The minimal surface $X_\mu^a(\xi)$ is not a string moving in a gravitational background, but a geometric representation of the gauge field components “unfolded” into their internal color dimensions.
3. **Conformal Invariance vs. Confinement:** Standard AdS/CFT begins with a conformal field theory; confinement requires breaking this symmetry “by hand” (e.g., via hard/soft walls). Our approach is the inverse: we begin with the Area Law as the fundamental physical input. The theory is inherently confining and non-conformal from the outset, with the mass scale set by the string tension σ .

Thus, our solution can be viewed as “Gauge Holography” rather than “Gravity Holography.” The minimal surface is a hologram of the loop, projected not into a fictitious gravitational dimension, but into the internal color space of the QCD vacuum. This avoids the need to map the glueball spectrum to bulk gravitons, allowing for the clear separation of static confinement and dynamic fluctuations discussed above.

Finally, we observe a striking parallel between the physical principle of color confinement and the geometric principle of holography. Just as

color confinement renders the internal color space unobservable—allowing us to interact only with gauge-invariant singlets—the holographic principle renders our 12D target space unobservable, allowing us to interact only with its boundary projection. In this framework, the physical Wilson loop C acts as the unique gauge-invariant observable, representing the projection of the hidden bulk geometry onto the physical world. The extra dimensions are not hidden by compactification, but by the very nature of the measurement process in a confining theory.

8. Conclusions

We have derived the high levels of $\bar{q}q$ meson mass spectrum associated with the confining area law in the quenched approximation. By solving the spectral equation for the Hodge-dual minimal surface, we obtain a linear Regge trajectory $M^2 \sim J$, consistent with the area law of confinement. Our confinement mechanism does not provide masses to glueballs; this would require further investigation.

The spacetime dimensionality $D = 4$ plays the unique role in this solution. The confinement mechanism relies fundamentally on the self-duality of the area derivative—a geometric property that exists exclusively in four dimensions. This stands in sharp contrast to *fundamental* bosonic string models, which require unphysical critical dimensions (e.g., $D = 26$) to maintain quantum consistency. While effective string theories can describe long flux tubes in $D = 4$, our result shows that the fundamental confining mechanism is a stable, non-vibrating minimal surface, exempt from the quantization anomalies of the fundamental Nambu-Goto string.

Our solution demonstrates that the confining surface is stable specifically in $D = 4$. This dimensionality constraint explains the absence of daughter trajectories in the resulting spectrum: the confining object is a minimal surface fixed by 4D geometry, not a fundamental string vibrating in higher embedding dimensions. The “missing” string modes are eliminated, leaving a clean linear Regge trajectory consistent with phenomenological observation.

Acknowledgements.—The author thanks colleagues at the Institute for Advanced Study for inspiring discussions.

References

[1] Y. Makeenko, A. Migdal, [Exact equation for the loop average in multicolor qcd](https://doi.org/10.1016/0370-2693(79)90131-X), Physics Letters B 88 (1) (1979) 135–137. doi:[url{https://doi.org/10.1016/0370-2693\(79\)90131-X}](https://doi.org/10.1016/0370-2693(79)90131-X).

URL [url{https://www.sciencedirect.com/science/article/pii/S037026937990131X}](https://www.sciencedirect.com/science/article/pii/S037026937990131X)

[2] Y. M. Makeenko, A. A. Migdal, Quantum chromodynamics as dynamics of loops, Nuclear Physics B 188 (1981) 269–316. doi:[10.1016/0550-3213\(81\)90105-2](https://doi.org/10.1016/0550-3213(81)90105-2).

[3] A. A. Migdal, Loop equations and $1/n$ expansion, Physics Reports 102 (4) (1983) 199–290. doi:[10.1016/0370-1573\(83\)90076-5](https://doi.org/10.1016/0370-1573(83)90076-5).

[4] A. Migdal, [Spontaneous quantization of the yang–mills gradient flow](https://doi.org/10.1016/j.nuclphysb.2025.117129), Nuclear Physics B 1020 (2025) 117129. doi:<https://doi.org/10.1016/j.nuclphysb.2025.117129>. URL <https://www.sciencedirect.com/science/article/pii/S0550321325003384>

[5] V. Kazakov, Z. Zheng, Bootstrap for finite n lattice yang-mills theory (2024). arXiv:[2404.16925](https://arxiv.org/abs/2404.16925).

[6] H. Poincaré, Sur l’uniformisation des fonctions analytiques, Acta Mathematica 31 (1) (1907) 1–63. doi:[10.1007/BF02415442](https://doi.org/10.1007/BF02415442).

[7] J. Douglas, [Solution of the problem of plateau](https://doi.org/10.2307/1989631), Transactions of the American Mathematical Society 33 (1) (1931) 263–321. doi:[10.2307/1989631](https://doi.org/10.2307/1989631). URL <https://doi.org/10.2307/1989631>

[8] T. Radó, On Plateau’s problem, Annals of Mathematics 31 (3) (1930) 457–469. doi:[10.2307/1968237](https://doi.org/10.2307/1968237).

[9] R. Gulliver, Regularity of minimizing surfaces of prescribed mean curvature, Annals of Mathematics 97 (2) (1973) 275–305. doi:[10.2307/1970845](https://doi.org/10.2307/1970845).

[10] B. White, The bridge principle for stable minimal surfaces, Calculus of Variations and Partial Differential Equations 4 (5) (1996) 411–425.

[11] B. Zwiebach, A First Course in String Theory, 2nd Edition, Cambridge University Press, 2009, Ch. 8, pp. 156–160, section 8.6: "The Rotating String". Derives the classical energy and angular momentum of the open string endpoint-to-endpoint, yielding the linear Regge trajectory $J = \alpha' E^2$.

[12] M. B. Green, J. H. Schwarz, E. Witten, Superstring Theory: Volume 1. Introduction, Cambridge Monographs on Mathematical Physics, Cambridge University Press, 1987.

[13] M. P. do Carmo, Differential Geometry of Curves and Surfaces, Prentice-Hall, 1976, see Section 2.5 for the Helicoid metric calculation.

[14] A. Hasenfratz, E. Hasenfratz, P. Hasenfratz, Roughening transition in lattice gauge theories in arbitrary dimension, Nuclear Physics B 180 (3) (1981) 353–367.

[15] M. Lüscher, G. Münster, P. Weisz, How thick are chromoelectric flux tubes?, Nuclear

- Physics B 180 (1) (1981) 1–12.
- [16] J. Fröhlich, The statistical mechanics of surfaces, in: L. Garrido (Ed.), Applications of Field Theory to Statistical Mechanics, Vol. 216 of Lecture Notes in Physics, Springer, Berlin, Heidelberg, 1985, pp. 31–57.
- [17] B. Durhuus, J. Fröhlich, T. Jonsson, Critical properties of constrained random surfaces, Nuclear Physics B 240 (4) (1984) 453–480.
- [18] K. J. Juge, J. Kuti, C. J. Morningstar, Fine structure of the qcd string spectrum, Phys. Rev. Lett. 90 (2003) 161601.
- [19] A. Enneper, Analytisch-geometrische untersuchungen, Zeitschrift für Mathematik und Physik 9 (1864) 96–125.
- [20] L. Euler, Methodus inveniendi lineas curvas maximi minimive proprietate gaudentes, Marc-Michel Bousquet, Lausanne & Geneva, 1744, chapter 5.
- [21] L. Henneberg, Über solche minimalflächen, welche eine vorgeschriebene ebene kurve zur geodätischen linie haben, Ph.D. thesis, Eidgenössische Technische Hochschule Zürich (1875).

Appendix A. General Theory: Spinor Factorization and Analytical Structure

The mathematical problem of minimization of the Dirichlet functional with Virasoro constraint in four dimensions is a well known problem in modern mathematics. Let us briefly summarize the existing theory.

Appendix A.1. Twistor Framework and the Klein Quadric

The fundamental constraint of the theory is the null condition on the holomorphic tangent vector of the minimal surface, $(f')^2 = \sum_{\mu=1}^4 (f'_\mu)^2 = 0$. Geometrically, this defines the *Klein Quadric* in the complexified tangent space $\mathbb{C}\mathbb{P}^3$. Using the isomorphism $SO(4, \mathbb{C}) \cong SL(2, \mathbb{C})_L \times SL(2, \mathbb{C})_R$, we map the vector f'_μ to a 2×2 matrix $f'_{ab} = f'_\mu (\sigma_\mu)_{ab}$. The null condition corresponds to $\det(f') = 0$, ensuring the matrix has rank 1. Thus, the tangent vector factorizes globally into a product of two spinors:

$$f'_{ab}(z) = \lambda_a(z)\mu_b(z) \quad (\text{A.1})$$

where λ_a and μ_b are meromorphic sections of spinor bundles over the worldsheet. This factorization linearizes the quadratic Virasoro constraint, replacing it with the problem of determining the analytic properties of the spinors.

Appendix A.2. Gauge Invariance and Birkhoff Factorization

The physical vector f' is invariant under the local complex gauge transformation:

$$\lambda_a(z) \rightarrow w(z)\lambda_a(z), \quad \mu_b(z) \rightarrow w^{-1}(z)\mu_b(z) \quad (\text{A.2})$$

where $w(z)$ is a meromorphic function. This redundancy is governed by the Birkhoff-Grothendieck theorem on the splitting of vector bundles over \mathbb{P}^1 . The gauge function $w(z)$ allows us to distribute the zeroes and poles between λ and μ , classifying solutions by integer topological indices (partial indices) related to the winding number of the gauge field required to regularize the spinors at infinity.

Appendix A.3. Analytic Structure via Plemelj Projection

The connection to the physical loop $C(\sigma)$ (where $\sigma = e^{i\theta}$) is achieved via the Plemelj-Sokhotski decomposition. We expand the loop coordinates into positive and negative frequency modes:

$$C(\sigma) = C_+(\sigma) + C_-(\sigma) = \sum_{n \geq 0} c_n \sigma^n + \sum_{n < 0} c_n \sigma^n \quad (\text{A.3})$$

If the loop is algebraic, $C_-(\sigma)$ extends to a rational function $C_-(z)$ in the complex plane $|z| > 1$. The poles of the spinor solution $f'(z)$ are dictated by the singularities of $C_-(z)$. Analytically, the problem is to find the "closest" null vector f' to the derivative $\partial_z C_+$. This is equivalent to finding a subspace W in the Sato Grassmannian that satisfies the isotropic condition and matches the boundary data.

Appendix A.4. Explicit Algebraic Solutions

The general theory of the spinor factorization predicts that rational choices for the sections $\lambda_a(z)$ and $\mu_b(z)$ generate algebraic minimal surfaces. These correspond to "Finite Gap" solutions where the algebraic curve has a finite genus. The distribution of poles between the spinors determines the topology and boundary behavior of the surface.

We illustrate this with four classical examples, reinterpreted in our spinor language: **1. The Enneper Surface (Polynomial Solution)**. This is the simplest solution with trivial topology (genus zero, one boundary at infinity), corresponding to polynomial spinors with a single pole at $z = \infty$.

$$\lambda(z) = \begin{pmatrix} 1 \\ z \end{pmatrix}, \quad \mu(z) = \begin{pmatrix} 1 \\ -z \end{pmatrix} \quad (\text{A.4})$$

The resulting null vector $f'(z) \sim (1 - z^2, i(1 + z^2), 2z, 0)$ integrates to a cubic polynomial map. This surface, discovered by Enneper in 1864 [19], represents the fundamental "ground state" of the algebraic solutions. **2. The Catenoid (Rational Solution with Poles)**. To generate a surface with the topology of an annulus (the only minimal

surface of revolution), one must introduce simple poles into the spinors.

$$\lambda(z) = \begin{pmatrix} z^{-1/2} \\ z^{1/2} \end{pmatrix}, \quad \mu(z) = \begin{pmatrix} z^{-1/2} \\ -z^{1/2} \end{pmatrix} \quad (\text{A.5})$$

Using the gauge freedom $\lambda \rightarrow w\lambda, \mu \rightarrow w^{-1}\mu$ with $w = z^{-1/2}$, we can redistribute the poles to find the standard rational form. Euler [20] originally proved the minimality of this surface, which corresponds to the physical shape of a soap film stretched between two rings. **3. The Henneberg Surface (Non-Orientable).** A more complex rational ansatz generates the Henneberg surface [21], which is a non-orientable minimal surface (a realization of the projective plane in 3D space). It arises from a rational map of degree 4:

$$\lambda(z) = \begin{pmatrix} 1 - z^{-2} \\ z - z^{-1} \end{pmatrix}, \quad \mu(z) = \begin{pmatrix} 1 \\ -1 \end{pmatrix} \quad (\text{A.6})$$

4. The Helicoid (Transcendental Solution).

The Helicoid is the locally isometric conjugate surface to the Catenoid. In the spinor formalism, it arises from the same meromorphic data but with a phase shift that exposes the period of the complex logarithm.

$$\lambda(z) = e^{i\pi/4} \begin{pmatrix} z^{-1/2} \\ z^{1/2} \end{pmatrix}, \quad \mu(z) = e^{i\pi/4} \begin{pmatrix} z^{-1/2} \\ -z^{1/2} \end{pmatrix} \quad (\text{A.7})$$

The resulting null vector possesses a pole with purely imaginary residue, $f'(z) \sim i/z$. Integration yields a logarithmic branch cut $f(z) \sim i \ln z$, corresponding to the multi-valued height function of the double helix ($X_3 \propto \Im(\ln z) = \theta$).